Biomaterials 33 (2012) 5841–5847

Contents lists available at SciVerse ScienceDirect

Biomaterials

journal homepage: www.elsevier.com/locate/biomaterials

High-throughput cellular screening of engineered ECM based on combinatorial polyelectrolyte multilayer films

Miloslav Sailer [a], Karen Lai Wing Sun [b], Ozzy Mermut [a], Timothy E. Kennedy [b,*], Christopher J. Barrett [a,*]

[a] Department of Chemistry, Program in NeuroEngineering, McGill University, 801 Sherbrooke St. W., Montreal, Quebec H3A 2K6, Canada
[b] Department of Neurology and Neurosurgery, Program in NeuroEngineering, Montreal Neurological Institute, 3801 University St., Montreal, Quebec H3A 2B4, Canada

ARTICLE INFO

Article history:
Received 16 February 2012
Accepted 2 May 2012
Available online 24 May 2012

Keywords:
Biocompatibility
Cell viability
Scaffold
Self assembly
Neural cell

ABSTRACT

The capacity to engineer the extracellular matrix is critical to better understand cell function and to design optimal cellular environments to support tissue engineering, transplantation and repair. Stacks of adsorbed polymers can be engineered as soft wet three dimensional matrices, with properties tailored to support cell survival and growth. Here, we have developed a combinatorial method to generate coatings that self assemble from solutions of polyelectrolytes in water, layer by layer, to produce a polyelectrolyte multilayer (PEM) coating that has enabled high-throughput screening for cellular biocompatibility. Two dimensional combinatorial PEMs were used to rapidly identify assembly conditions that promote optimal cell survival and viability. Conditions were first piloted using a cell line, human embryonic kidney 293 cells (HEK 293), and subsequently tested using primary cultures of embryonic rat spinal commissural neurons. Cell viability was correlated with surface energy (wettability), modulus (matrix stiffness), and surface charge of the coatings.Our findings indicate that the modulus is a crucial determinant of the capacity of a surface to inhibit or support cell survival.

1. Introduction

The extracellular matrix (ECM) is a complex mixture of proteins, polysaccharides, and growth factors that provide structural support and mediate cellular function. Synthetically mimicking natural ECM is a major goal of tissue engineering for therapeutic applications such as restoring, maintaining, or enhancing tissue function and for *in-vivo* diagnostic applications such as testing for drug toxicity and measuring metabolism. The complexity of cell-ECM interactions makes understanding the underlying principles of matrix function paramount to advancing the field [1]. Two main categories important for anchorage-dependent cellular development have been identified; the biological ECM protein interactions [2,3] that function through *specific* receptor-ligand signaling mechanisms, and physical *non-specific* interactions [4] that are dependent on the structural properties of the substrate. Although the bulk of research has focused on specific signaling mechanisms, there is growing evidence suggesting that non-specific physical properties of the substrate such as surface charge [5–7], surface energy [8–12], and the modulus of the coating [13–20], play crucial roles in cellular structure and function. However, the effects of these physical properties on cell behavior are usually measured independently of each other. This inherently leads to confounding effects as some properties are not accounted for, limiting the value of the result. The challenge to achieving a better understanding of substrate property effects stems from the large parameter space; however, it is tedious to handle such complexity with a conventional one sample approach. High-throughput combinatorial experimental strategies allow for a large number of variables to be addressed simultaneously and have been used to develop materials such as biodegradable polymers [21], polymeric supports for organic synthesis [22], sensors for herbicides [23], and non-cytotoxic materials [24,25].

Ideal candidates for making combinatorial substrates are charged polymers called polyelectrolytes that can be sequentially layered through an alternating layer-by-layer method to make stacks of polyelectrolytes called a polyelectrolyte multilayer (PEM) [26,27]. A major advantage of PEMs is that they can be made from any charged water-soluble polymer with any number of layers, and each layer can have a tunable internal architecture and density. The two most basic and well-studied polyelectrolytes used to make PEMs are poly (allylamine hydrochloride) (PAH), a carbon backbone polymer with pendent amine groups (Fig. 1A), and poly (acrylic acid) (PAA), which has pendent carboxylic acid groups (Fig. 1B). The build-up is initiated by submerging a negatively charged substrate into a solution of PAH. The positively charged

* Corresponding authors.
E-mail address: Chris.Barrett@mcgill.ca (C.J. Barrett).

0142-9612/$ – see front matter © 2012 Elsevier Ltd. All rights reserved.
doi:10.1016/j.biomaterials.2012.05.001

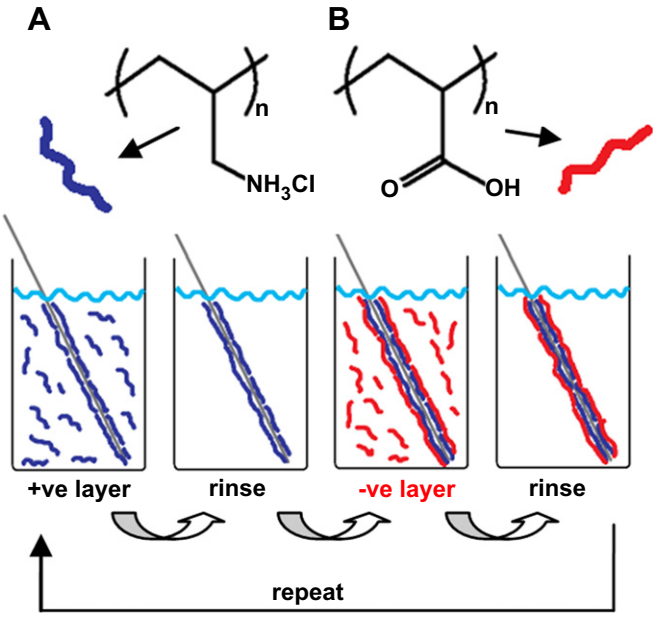

Fig. 1. Molecular structures of A) Poly(allylamine hydrochloride) and B) Poly(acrylic acid) and C) an illustration of a general 1-b-l PEM fabrication process.

polymer self-assembles onto the surface, masking and reversing the negative charge and making the surface positively charged (Fig. 1C). The positively charged coated substrate is then submerged into a solution of PAA and similarly a second layer of polymer is deposited onto the substrate, reverting the charge back to negative. This process is repeated to generate a coating that is held strongly together by many electrostatic cross-links. Additionally, since PAA and PAH are weak polyions, the degree of charge per chain (i.e. $-COO^-/-COOH$ and $-NH_2/-NH_3^+$ ratios) is influenced by the pH of the deposition solution, which provides control over the conformation (e.g. linear or loopy) of the polymer chains making up the coatings. By changing the pH of the two polymer solutions, the layer-by-layer method provides control over physical properties such as the surface charge, surface energy, thickness, water content, and the modulus of the coatings that are important for 'bioactivity'. Such tunability makes PEMs attractive materials that have found their way into a wide range of applications, including optical coatings [28], macromolecular encapsulation [29,30], and non-cytotoxic films [31]. PEMs with these specific properties are typically made individually; however, due to the large assembly parameter space, optimizing these precisely tailored coatings can be prohibitively time-consuming and expensive.

As an initial step toward engineering enhanced extracellular environments, we developed a high-throughput combinatorial instrument for the fabrication of gradient PEM films. The instrument works by continuously altering the amount of charge of solvated PAA and/or PAH chains as the film is layered across the plane, which is done by varying the pH of the adsorption bath. By rotating the substrate ±90 ° after each layer is deposited, 2D thickness-gradient films were made, representing on just a few square centimeters the equivalent parameter space of many thousands of individual uniform films. The films were then characterized under water by determining the average thickness, surface energy, and modulus across the entire area of the film. The capacity of a surface to support cell growth was then determined by examining the survival of HEK 293 cells and embryonic rat neurons, and related to the physical properties at that *x* and *y* location on the film.

2. Methods

2.1. Assembly of 2D gradient pH films

7 × 7 cm cleaved silicon wafers (University Wafer, San Jose, CA) were gradually immersed into a solution of poly(allyl amine hydrochloride) (PAH, MW 65,000, Sigma Aldrich) at a varying pHs with stirring. The resultant film was then rinsed, rotated by 90°, and gradually immersed into a solution of poly(acrylic acid) (PAA, MW = 100,000, Sigma Aldrich) at a varying pHs. The film was rinsed and the process was repeated until the desired number of layers was deposited.

2.2. Thickness measurements

The thickness of the gradient multilayer films was measured using single wavelength (633 nm) null-ellipsometry (Optrel Multiskop, Germany) fixed at 70 ° to the normal. For underwater ellipsometry, films were submerged in water for 24 h prior to measurement to ensure full hydration, as per the *in-situ* techniques described previously by our group [32–34]. Films were placed on a mobile stage (Δ 1 mm) and Δ and ψ measurements were taken at 5 mm intervals. These measurements were then processed using an appropriate model (water ($n = 1.33$)// film ($t = x$, $n = x$)//SiO_2 ($t = 2.3$ nm, $n = 1.54$)//Si ($n = 3.42$, $k = -0.011$), to obtain thickness and refractive index values.

2.3. Cell survival assays

Human embryonic kidney 293 (HEK 293) cells were cultured in Dulbecco's modified Eagle medium (DMEM, Invitrogen) supplemented with 100 unit/mL penicillin G (Invitrogen), 100 μg/mL streptomycin (Invitrogen), and 10% fetal bovine serum (Invitrogen). Cultured cells were incubated in a 5% CO_2 and 37 °C humidified incubator. Spinal commissural neurons were isolated from embryonic day 13.5 (E13.5) Sprague–Dawley rat embryos and cultured in Neurobasal medium (Invitrogen) supplemented with 100 unit/mL penicillin G, 100 μg/mL streptomycin, 2 mM GlutaMAX-1 (Invitrogen) and 10% fetal bovine serum. After 16–24 h in culture, the medium was replaced with Neurobasal medium supplemented with 100 unit/mL penicillin G, 100 μg/mL streptomycin, 2 mM GlutaMAX-1 and 2% B-27 (Invitrogen). For adhesion and growth assays, 15,000 HEK 293 cells/cm^2 and ~1 million neurons were plated per PEM film coated silicon wafers. HEK 293 cells following 1 day *in vitro* (DIV) and spinal commissural neurons at 2 DIV were fixed with 4% paraformaldehyde (PFA, Fisher Scientific) and 0.1% gluteraldehyde (Sigma) for 60 s and then blocked with 3% heat inactivated horse serum (HS, Invitrogen) and 0.1% Triton X-100 (Fisher Scientific). Cells were stained with 0.8 unit/mL Alexa 488 coupled Phalloidin (Invitrogen) and 500 ng/mL Hoechst 33258 (Invitrogen). Films were cover slipped using FluoroGel (Electron Microscopy Sciences).

2.4. Cell imaging and counting

Cells were imaged using an Axiovert 100 inverted fluorescence microscope (Carl Zeiss Canada, Toronto, ON) with a Magnafire CCD camera and MagnaFire 4.1C imaging software (Optronics, Goleta, CA). Images were captured at positions equivalent to thickness measurement locations (controlled by an x-y Δ1 mm stage). The number of cells was quantified by counting Hoechst positive nuclei using ImageJ software (U. S. National Institutes of Health, Bethesda, Maryland, USA). The macro used for cell counting consisted of conversion to a 16-bit picture format, background subtraction, threshold adjustment to exclude background, conversion to binary, and a cell count/cell area calculation. The same macro was used for all images to ensure consistent counts. To measure the surface area of embryonic spinal commissural neurons, cells were stained with fluorescently labeled phalloidin to visualize F-actin and total cell area per image calculated.

2.5. Modulus measurements using Atomic force Microscopy (AFM)

Force measurements of the multilayer films were performed using an AFM in force calibration mode (Nanoscope Version 3A, Digital Instruments), using protocols previously described by our group [35]. The multilayer surface and the tip were brought together in a fluid cell at room temperature. Silicon nitride probes were used (radius = 20–60 nm) with a manufacturer specified force constant, *k*, of 0.12 N/m. All elasticity measurements of the films were performed with the same AFM tip; thus, no calibration for the absolute spring constant of the tip was done. The AFM detector sensitivity was calibrated by obtaining a force curve on a baer substrate and determining the slope of the linear portion of the data after contact. Obtaining force curves of the multilayer film involved bringing the tip in close contact with the surface in aqueous media and obtaining force measurements after allowing the system to equilibrate for 10 min, or until reproducible curves were observed. The rate of the indentation cycle was kept constant at 0.2 Hz. For elasticity measurements, four replicate measurements of the tip deflection as a function of the piezo z-position were acquired with the unmodified AFM tip.

2.6. Surface energy measurements

Surface energy measurements were performed using the sessile drop technique by carefully depositing a droplet of diiodomethane (CH_2I_2) (≈3 μl) on the surface of the films submerged in water and measuring the contact angle. An EHD©KamPro02 high resolution digital camera mounted on an adjustable stage was used to acquire images of the droplets that were then analyzed with the Youngs-Dupree model. Contact angle measurements were converted to surface energies using the Fowkes approach [36].

3. Results and discussion

3.1. Instrument design

In order to generate films through layer-by-layer self assembly, an instrument was designed to enable quick generation of gradients and combinatorial coatings of any size using any polyelectrolyte. The instrument uses two pumps and two solutions that enable the experimenter to build a PEM film spanning all possible pH combinations (Fig. 2A). The device works by having one solution that contains H^+ or ^-OH ions of a desired concentration that will affect the polyelectrolytes properties in solution, such as the amount of charge. The ion solution is pumped at any desired rate into the polyelectrolyte solution whilst simultaneously that polyelectrolyte solution is pumped into the container where deposition will occur on the substrate. Since the height of the solution level in the container corresponds to the position of adsorption on the substrate, the secondary flow rate, along with the size of the container, allows for the lateral resolution of the deposition to be tuned. Because the film is exposed to changing pH, this technique is only suitable for systems where layer adsorption is irreversible, and the underlying film architecture is unaffected, irrespective of the pH of the solution.

3.2. 2D combinatorial gradient PEM films

The gradient instrument was used to fabricate films by varying the deposition pH of PAA from 3 to 6.5 on one axis and varying the deposition pH of PAH from 11 to 7 on the other axis— pH regimes that pass through the pKa and pKb regions of PAA and PAH respectively providing thousands of different combinations of deposition charge ratios.

The 2-dimensional average thickness map illustrated in Fig. 3A shows a high dependence of average layer thickness to assembly pH. Since the number of layers across the entire film is constant, the change in thickness results mainly from the difference in the length of polymer loops in each layer. For example, a polymer in solution with high charge will form highly interpenetrated flat layers, whereas a polymer with low charge will adopt dense conformational loops extending away from the surface. Therefore, it can be generalized that the thinnest regions of the film contain tightly packed PAH and PAA polymers, orthogonal regions of moderate thickness contain a mixture of non-loopy and loopy polymers, and the thickest part of the film is composed of loopy polymers of PAA and PAH.

When immersed in water, the film swells. The degree of swelling (underwater thickness − dry thickness/dry thickness) varied across different areas of the film and was directly correlated with the refractive index of the film, a measure of density [32–34]. The areas made with loopy polymers had the lowest refractive index (Fig. 3B) and swelled the most (Fig. 3C). These loopy regions contain an excess amount of free $-NH_3^+$ in the PAH layer and $-COO^-$ in the PAA layer (i.e. extrinsically charge compensated charged groups) that are not electrostatically bound to a complementary polymer chain. Since there are few ionic cross-links in these regions, water diffuses into the film and has room to expand, and even expanded by ~50% or more in these loopy regions

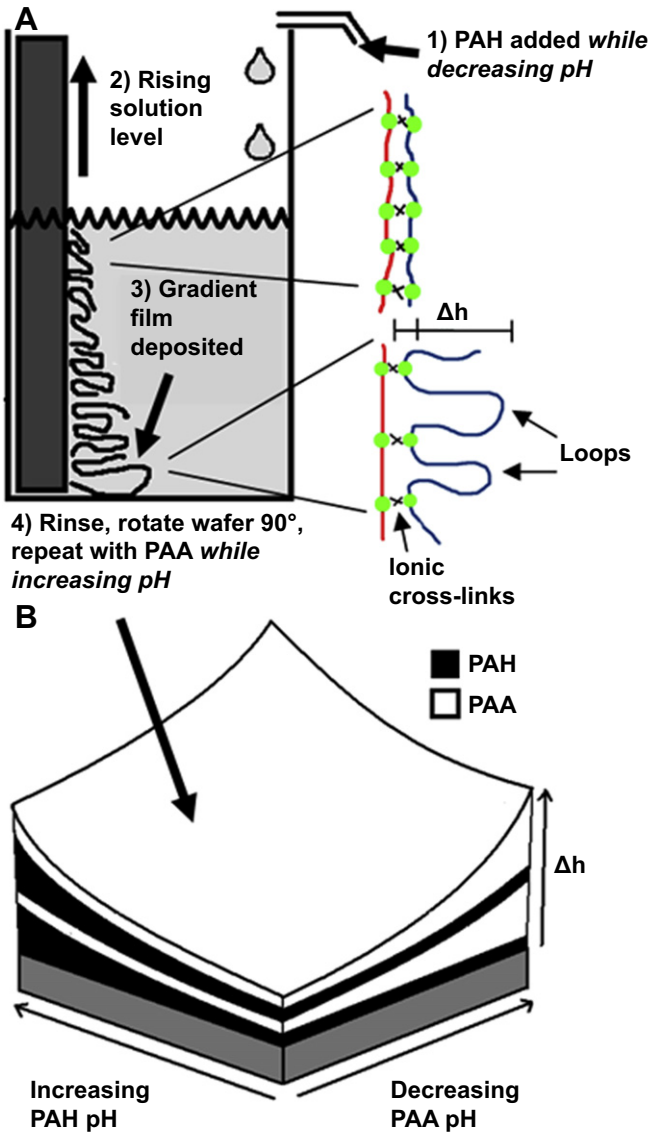

Fig. 2. A) As the solution level rises and the polyelectrolyte is deposited on the substrate, the conformation of the polyelectrolyte changes due to the changing pH of the solution resulting in a thicker film on one end and a thinner film on the other. B) An illustration of what the thickness profile would look like (shown after 4 layers) after rotating by ±90 ° and rinsing after each deposition step.

[32–34]. In the opposite situation, the thinnest regions have very little non-complexed charges and are tightly bound, so naturally swell the least.

Surface energy is the amount of 'free energy' of a surface that can be used to do work. In water, the higher the surface energy, the more hydrophilic the surface is. Usually surface energy is measured by carefully placing drops of water and diiodomethane onto a surface to determine both the polar and dispersive components of that surface energy. However, since the films absorb water and increase in thickness, we expect the surface energy to change when the film is filled with water. Unfortunately, it is difficult to measure the total surface energy of a film underwater since one of the two drops required to determine total surface energy must be polar, water insoluble, and more dense than water, and such a combination is not easily achievable. However, using diiodomethane, it is possible to measure the dispersive component of surface energy, which still provides information about the hydrophobicity of the surface underwater. Fig. 3D depicts the dispersive component of

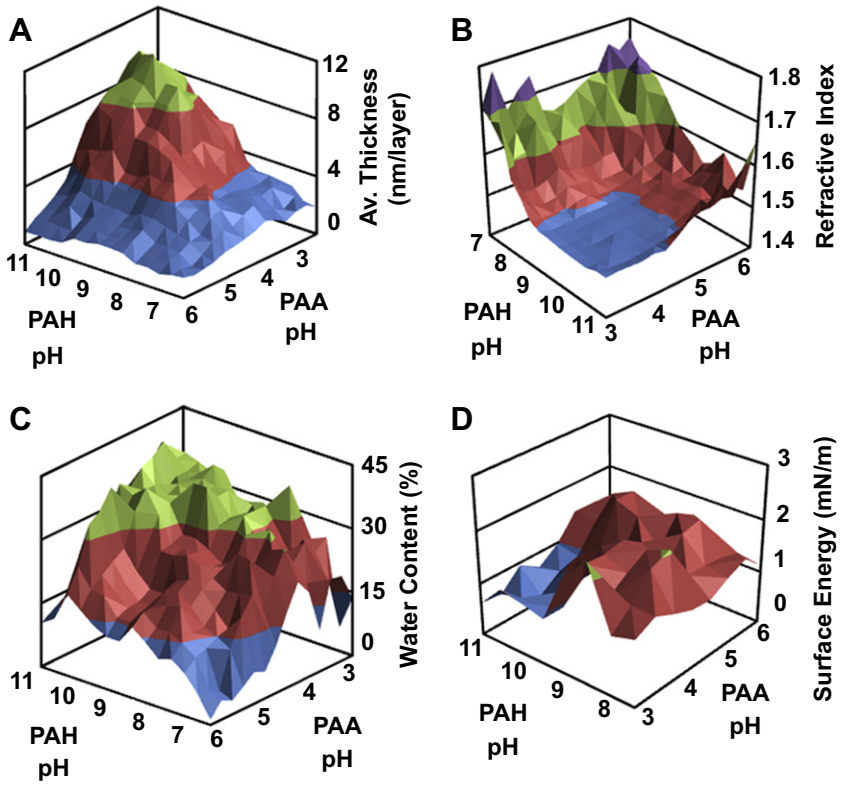

Fig. 3. A 10 layer PEM film ($(PAH/PAA)_5$) built between a PAA pH range of 3–6 and a PAH pH range of 11-8 with surface maps of A) underwater thickness, B) refractive index ellipsometry measurements, C) water content (underwater thickness − dry thickness(data not shown)/dry thickness) and D) the dispersive component of surface energy calculated using underwater sessile diiodomethane drop contact angle measurements and the Fowkes method.

surface energy across the film and reveals that the thicker, low density films are more hydrophilic, which is consistent with them containing almost 50% water.

3.3. Assessing biocompatibility using the HEK 293 cell line

Initially, several films were fabricated at extreme pH conditions with opposite surface charges to determine the extent to which PEMs influence cell adhesion. To investigate the response of cells to these surfaces, we first used HEK 293 cells, a cell line routinely used in many laboratories. Fig. 4A,B depict the morphology of HEK 293 cells stained with Phalloidin to visualize F-actin when plated on thin PEM films made using polyelectrolytes with high charge density. Following 48 h in culture, HEK 293 cells were viable on these surfaces and exhibited a well defined cytoskeleton, demonstrating biocompatibility. Cells on the positively charged coatings with an average thickness of 0.25 nm/layer revealed no apparent difference in morphology compared to cells grown on the negatively charged film. In contrast, no cells remained when plated on thick PEM films (Fig. 4C,D) fabricated using polyelectrolytes with low charge. At this extreme thickness, only cell debris was detected. No difference in cell morphology was detected between positively charged films with an average thickness of 9.3 nm/layer (Fig. 4C) and negatively charged films with an average thickness of 8.5 nm/layer (Fig. 4D), similar to the thin films. Since modulus is generally negatively correlated with average thickness in the same polyelectrolyte multilayer system as shown with our neuronal studies (i.e. films with a relatively low modulus have thicker layers than films with a high modulus) [35], these findings provide strong evidence that the role of the modulus of the film is more critical than the surface charge in influencing cell morphology. Indeed, this is consistent with an established literature which documents that the modulus of a substrate is crucial in determining its biocompatibility [17–24].

The average thickness profiles of the negatively and positively charged combinatorial films exhibited variable numbers of cells after 48 h in culture (Fig. 5A,B). Using these new combinatorial films, we determined that HEK 293 cells survive best on PEM films fabricated using a low PAH pH and a low PAA pH. Conversely, films fabricated with a low PAA pH and a high PAH pH are the substrates least supportive of cell survival. Overall, areas of highest average thickness of ~13.3 nm/layer exhibited the fewest surviving HEK 293 cells. Our findings indicate that HEK 293 cells survive best on films with an intermediate average thickness of ~3 nm/layer and therefore an intermediate modulus. To investigate the effect of surface charge across all possible pH assembly conditions, one of the films was terminated with a positively charged polyelectrolyte (Fig. 5A) and another with a negatively charged polyelectrolyte (Fig. 5B). Following 48 h in culture, the positively charged surfaces had approximately twice the number of cells than the negatively charged surfaces. Thus, both surface charge and modulus contribute to the biocompatibility of surfaces for HEK 293 cells, with the latter being more significant. The similarity of the overall morphology of HEK 293 cells on either negatively or positively charged films (Fig. 4A,B and Fig. 5A,B) suggests that once a cell has successfully adhered to a surface, an event strongly influenced by surface charge, the morphological response of the cells is then influenced by the modulus.

3.4. Assessing film biocompatibility for neuronal survival and differentiation

Mammalian central nervous system (CNS) neurons isolated from rat embryos are widely used for neurobiogical studies [37], but remain a relatively demanding cell type to maintain *in vitro*.

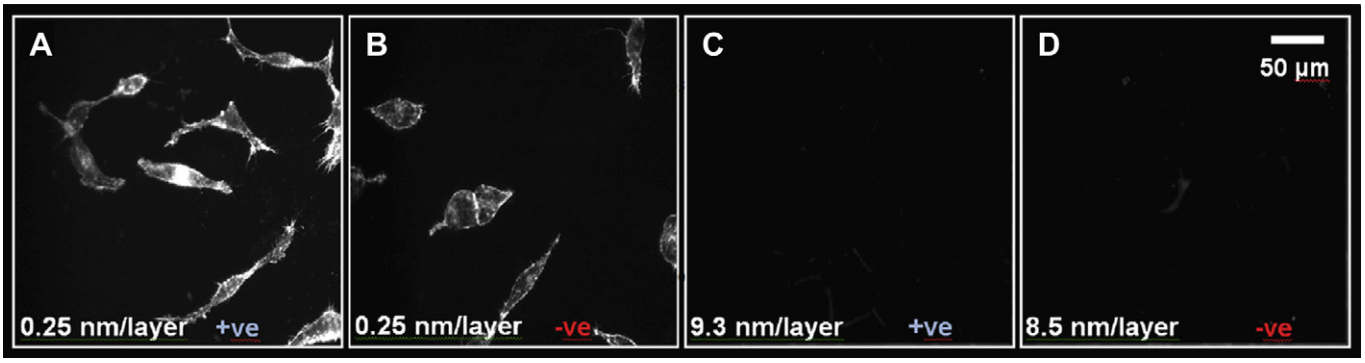

Fig. 4. HEK 293 cell morphology (actin filament stain) using a 40X objective lens after 2DIV. A) A positively charged film assembled at PAA pH 9.5 and PAH pH 3 with an average thickness of 0.25 nm/layer. B) A negatively charged film assembled at PAA pH 9.5 and PAH pH 3 with an average thickness of 0.25 nm/layer. C) A positively charged film assembled at PAA pH 3.0 and PAH pH 7.5 with an average thickness of 9.3 nm/layer. D) A negatively charged film assembled at PAA pH 3.0 and PAH pH 7.5 with an average thickness of 8.5 nm/layer.

Here we isolated and cultured embryonic rat spinal commissural neurons, a well characterized type of spinal sensory interneuron [38]. Plating commissural neurons on PEMs that were produced using different pH conditions resulted in similar morphological changes as previously observed for the HEK 293 cells. Films made from polymers with high charge density generated surfaces with a high modulus and an average thickness of ~3 nm/layer. Neurons grown in these conditions projected multiple neurites from their cell bodies (Fig. 6A,B). In contrast, films made from low charge density polymers generated a surface with a low modulus and an average thickness of ~12.6 nm/layer on which only cell debris were detected (Fig. 6C,D). Similar to the HEK 293 cells, no difference in neuronal morphology was detected when cells were plated on negatively (Fig. 6A,C) or positively (Fig. 6B,D) charged surfaces.

Fig. 7A presents a compilation of images across the surface of a 2D combinatorial positively charged film, illustrating regional differences in cell viability on the film. Considering the physical properties of the film shown in Fig. 7B,D, the transition between regions that are permissive and non-permissive for cell survival is abrupt and occurs within 1 pH unit with no cells detected at a PAA assembly pH range of 4–6 with a complementary PAH assembly pH range of 8–10.5 (Fig. 7E). These pH conditions correspond to an average thickness of ~10 nm/layer with the transition occurring between 8.5 and 10 nm/layer, which corresponds to a modulus range of 500–800 kPa. No cells survived on film with a modulus below 500 kPa. Interestingly, in regions exhibiting a modulus of over ~2500 kPa at the thinnest regions of the film, a reduction in cell viability was detected, with the thinnest regions also being non-permissive (Fig. 7A). Indeed, an intermediate modulus appears to be optimal for both HEK 293 cells and commissural neurons. No correlation was detected between surface energy and cell viability. This may be due to surface energy variations across the film being relatively small or that surface energy influences may be overshadowed by the effects of differences in modulus across the entire film.

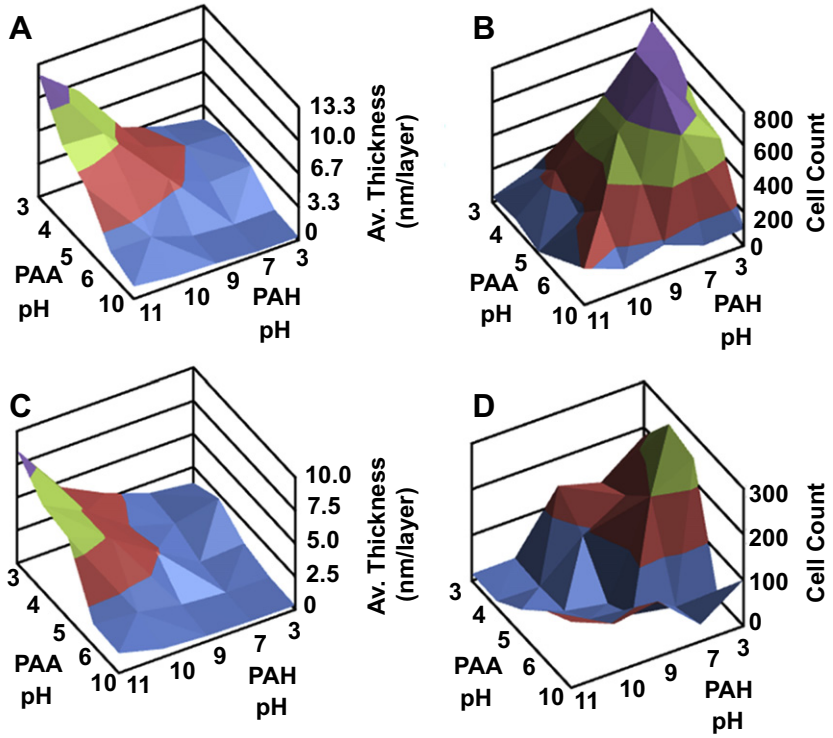

Fig. 5. HEK 293 cells were incubated for 2DIV on a A) positively charged 2D PEM film which resulted in a B) cell survival distribution, and on a C) negatively charged 2D PEM films which resulted in a D) cell survival distribution.

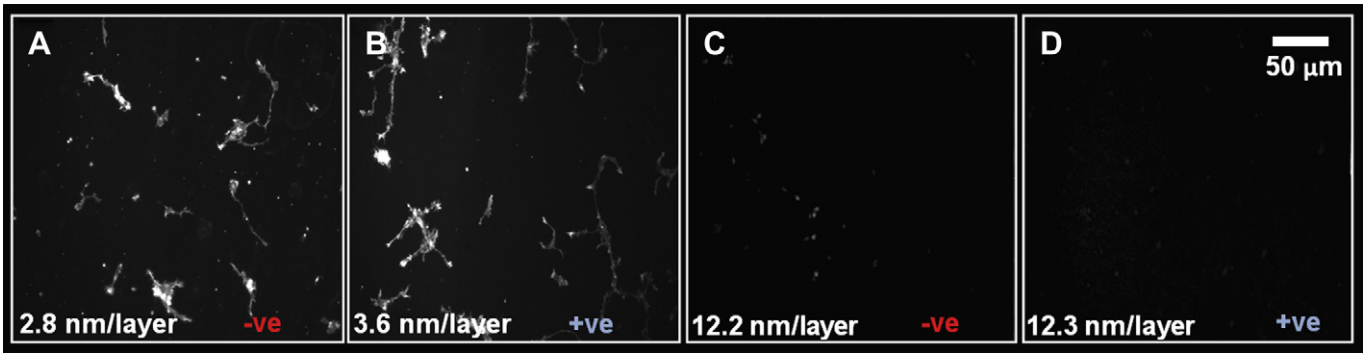

Fig. 6. Embryonic rat spinal commissural neuron morphology (actin filament stain) using a 40X objective lens after 2DIV. A) A positively charged film assembled at PAA pH 6 and PAH pH 7 with an average thickness of 2.8 nm/layer. B) A negatively charged film assembled at PAA pH 6 and PAH pH 7 with an average thickness of 3.6 nm/layer. C) A positively charged film assembled at PAA pH 4.5 and PAH pH 9.5 with an average thickness of 9.3 nm/layer. D) A negatively charged film assembled at PAA pH 4.5 and PAH pH 9.5 with an average thickness of 12.3 nm/layer.

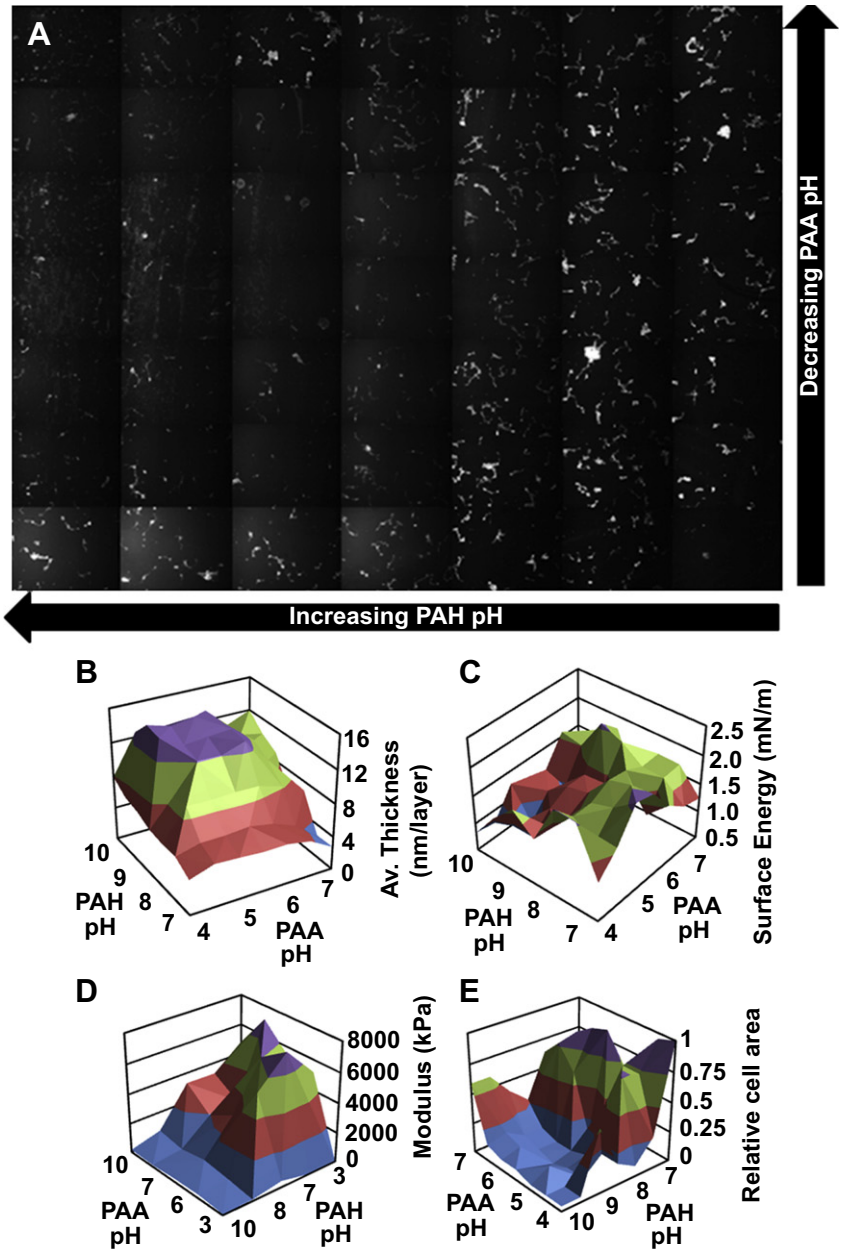

Fig. 7. A) A compilation of images of embryonic rat spinal commissural neuron morphologies (actin filament stain) using a 40X objective lens after 2DIV with corresponding 2D physical property maps of B) average thickness, C) dispersive surface energy, and D) modulus. Furthermore, E) cell areas were calculated, normalized, and plotted as a map of relative cell area, reflecting the number of viable cells distributed across the surface.

4. Conclusions

In summary, a new PEM fabrication technique was developed to enable the production of a variety of PEM gradient films. With these films, we screened the survival of HEK 293 and embryonic rat spinal commissural neurons based on PEM pH assembly conditions and correlated them to the physical properties of the film. Both cell types prefer an environment of an intermediate modulus composed of moderately charged polyelectrolytes. Moreover, it was found that the modulus of the material plays a more crucial role than surface energy or surface charge in determining the biocompatibility of a surface. These films provide an initial step toward attaining an in-depth understanding of cell–surface interactions, with the goal of unraveling the influence of fundamental physicochemical attributes on cell survival.

Acknowledgments

Supported by operating grant #FRN79513 to TEK from the Canadian Institutes of Health Research (CIHR), a New Emerging Team grant from CIHR, and a NSERC CREATE team grant to TEK and CJB in support of the McGill Program in NeuroEngineering. KLWS was supported by a Jeanne-Timmins Costello Graduate Fellowship. TEK is a Killam Foundation Scholar and holds a Chercheur National award from the Fonds de la Recherche en Santé du Québec.

References

[1] MacArthur BD, Oreffo ROC. Bridging the gap. Nature 2005;433(7021):19.
[2] Hynes RO. The extracellular matrix: not just pretty fibrils. Science 2009; 326(5957):1216–9.
[3] Bowers SLK, Banerjee I, Baudino TA. The extracellular matrix: at the center of it all. J Mol Cell Cardiol 2010;48(3):474–82.
[4] Lee MH, Brass DA, Morris R, Composto RJ, Ducheyne P. The effect of non-specific interactions on cellular adhesion using model surfaces. Biomaterials 2005;26(14):1721–30.
[5] Seo J, Lee H, Jeon J, Jang Y, Kim R, Char K, et al. Tunable layer-by-layer polyelectrolyte platforms for comparative cell assays. Biomacromolecules 2009; 10(8):2254–60.
[6] Yu DG, Lin WC, Lin CH, Yeh YH, Yang MC. Construction of antithrombogenic polyelectrolyte multilayer on thermoplastic polyurethane via layer-by-layer self-assembly technique. J Biomed Mater Res B Appl Biomater 2007;83B(1): 105–13.
[7] Khorasani MT, MoemenBellah S, Mirzadeh H, Sadatnia B. Effect of surface charge and hydrophobicity of polyurethanes and silicone rubbers on l929 cells response. Colloids Surf B Biointerfaces 2006;51(2):112–9.
[8] Tianyi Y, Zaman MH. Free energy landscape of receptor-mediated cell adhesion. J Chem Phys 2007;126(4):045103.
[9] Liu X, Lim JY, Donahue HJ, Dhurjati R, Mastro AM, Vogler EA. Influence of substratum surface chemistry/energy and topography on the human fetal osteoblastic cell line hfob 1.19: Phenotypic and genotypic responses observed in vitro. Biomaterials 2007;28(31):4535–50.
[10] Satriano C, Carnazza S, Guglielmino S, Marletta G. Surface free energy and cell attachment onto ion-beam irradiated polymer surfaces. Nucl Instrum Meth B 2003;208:287–93.
[11] Harnett EM, Alderman J, Wood T. The surface energy of various biomaterials coated with adhesion molecules used in cell culture. Colloids Surf B Biointerfaces 2007;55(1):90–7.
[12] Lampin M, Warocquier-Clérout R, Legris C, Degrange M, Sigot-Luizard MF. Correlation between substratum roughness and wettability, cell adhesion, and cell migration. J Biomed Mater Res 1997;36(1):99–108.
[13] Huang J, Peng X, Xiong C, Fang J. Influence of substrate stiffness on cell-substrate interfacial adhesion and spreading: a mechano–chemical coupling model. J Colloid Interface Sci 2011;355(2):503–8.
[14] Mehrotra S, Hunley SC, Pawelec KM, Zhang L, Lee I, Baek S, et al. Cell adhesive behavior on thin polyelectrolyte multilayers: cells attempt to achieve homeostasis of its adhesion energy. Langmuir 2010;26(15):12794–802.
[15] Lichter JA, Thompson MT, Delgadillo M, Nishikawa T, Rubner MF, Van Vliet KJ. Substrata mechanical stiffness can regulate adhesion of viable bacteria. Biomacromolecules 2008;9(6):1571–8.
[16] Ren K, Crouzier T, Roy C, Picart C. Polyelectrolyte multilayer films of controlled stiffness modulate myoblast cell differentiation. Adv Funct Mater 2008;18(9): 1378–89.
[17] Discher DE, Janmey P. Wang Y-l. Tissue cells feel and respond to the stiffness of their substrate. Science 2005;310(5751):1139–43.
[18] Schneider A, Francius G, Obeid R, Schwinté P, Hemmerlé J, Frisch B, et al. Polyelectrolyte multilayers with a tunable young's modulus: influence of film stiffness on cell adhesion. Langmuir 2005;22(3):1193–200.
[19] Yeung T, Georges PC, Flanagan LA, Marg B, Ortiz M, Funaki M, et al. Effects of substrate stiffness on cell morphology, cytoskeletal structure, and adhesion. Cell Motil Cytoskeleton 2005;60(1):24–34.
[20] Gray DS, Tien J, Chen CS. Repositioning of cells by mechanotaxis on surfaces with micropatterned young's modulus. J Biomed Mater Res A 2003;66A(3): 605–14.
[21] Brocchini S, James K, Tangpasuthadol V, Kohn J. Structure-property correlations in a combinatorial library of degradable biomaterials. J Biomed Mater Res 1998;42(1):66–75.
[22] Gravert DJ, Datta A, Wentworth P, Janda KD. Soluble supports tailored for organic synthesis: Parallel polymer synthesis via sequential normal/living free radical processes. J Am Chem Soc 1998;120(37):9481–95.
[23] Takeuchi T, Fukuma D, Matsui J. Combinatorial molecular imprinting: An approach to synthetic polymer receptors. Anal Chem 1998;71(2):285–90.
[24] Meredith JC, Sormana JL, Keselowsky BG, García AJ, Tona A, Karim A, et al. Combinatorial characterization of cell interactions with polymer surfaces. J Biomed Mater Res A 2003;66A(3):483–90.
[25] Kennedy SB, Washburn NR, Simon JCG, Amis EJ. Combinatorial screen of the effect of surface energy on fibronectin-mediated osteoblast adhesion, spreading and proliferation. Biomaterials 2006;27(20):3817–24.
[26] Decher G, Schmitt J. Fine-tuning of the film thickness of ultrathin multilayer films composed of consecutively alternating layers of anionic and cationic polyelectrolytes. In: Helm C, Lösche M, Möhwald H, editors. Prog Coll Pol Sci S. Berlin/Heidelberg: Springer; 1992. p. 160–4.
[27] Decher G. Fuzzy nanoassemblies: toward layered polymeric multicomposites. Science 1997;277(5330):1232–7.
[28] Hiller JA, Mendelsohn JD, Rubner MF. Reversibly erasable nanoporous anti-reflection coatings from polyelectrolyte multilayers. Nat Mater 2002;1(1): 59–63.
[29] Dorris AC, Douglas KL, Tabrizian M, Barrett CJ. Control of DNA incorporation into nanoparticles with poly(l-lysine) multilayers. Can J Chem 2008;86(12): 1085–94.
[30] Schüler C, Caruso F. Decomposable hollow biopolymer-based capsules. Biomacromolecules 2001;2(3):921–6.
[31] Mendelsohn JD, Yang SY, Hiller JA, Hochbaum AI, Rubner MF. Rational design of cytophilic and cytophobic polyelectrolyte multilayer thin films. Biomacromolecules 2002;4(1):96–106.
[32] Tanchak OM, Barrett CJ. Swelling dynamics of multilayer films of weak polyelectrolytes. Chem Mater 2004;16(14):2734–9.
[33] Tanchak OM, Yager KG, Fritzsche H, Harroun T, Katsaras J, Barrett CJ. Water distribution in multilayers of weak polyelectrolytes. Langmuir 2006;22(11): 5137–43.
[34] Tanchak OM, Yager KG, Fritzsche H, Harroun T, Katsaras J, Barrett CJ. Ion distribution in multilayers of weak polyelectrolytes: a neutron reflectometry study. J Chem Phys 2008;129(8):084901.
[35] Mermut O, Lefebvre J, Gray DG, Barrett CJ. Structural and mechanical properties of polyelectrolyte multilayer films studied by afm. Macromolecules 2003;36(23):8819–24.
[36] Fowkes FM. Attractive forces at interfaces. Ind Eng Chem 1964;56(12):40–52.
[37] Banker G, Goslin K. Culturing nerve cells. 2 ed. Bradford Book; 1998.
[38] Moore SW, Kennedy TE. Dissection and culture of embryonic spinal commissural neurons. Current protocols in neuroscience. John Wiley & Sons, Inc.; 2001.